

Electrolytic and Thermal Bubble Generation Using AC Inductive Powering

Bo K. Choi, Min Ma, Christopher White, and Chang Liu
Micro Actuator and Sensor Systems (MASS) Group
University of Illinois at Urbana-Champaign, Urbana, IL, 61801

ABSTRACT

We present the characteristics of thermal bubble generation under alternating current, AC bias condition. Micro thermal bubble generators have been fabricated and tested. Dimensions of polysilicon resistors tested are $40 \times 2 \times 0.5 \mu\text{m}$ and $40 \times 6 \times 0.5 \mu\text{m}$. Each device shows very distinct and unique characteristics under AC bias. The threshold power for bubble generation is a function of the input frequency, waveform, and the dimension of the resistor. Thermal bubble generation using AC bias allows having energy-efficient inductive powering of wireless pneumatic actuators for micro fluidic applications. On the basis of the pool boiling theory and the results from the DC power input, we expected constant threshold power with respect to input frequency and wave form. However, we have found that for $2\mu\text{m}$ -width resistor, minimum threshold power to generate a bubble occurs at 5.3 MHz. A peak of the threshold power occurs at frequency around 4 MHz (Sine wave). Lower threshold power is required for square wave. A different characteristic curve of threshold power is shown after release. Also, the $6\mu\text{m}$ -width unreleased resistor shows a different input power characteristics from unreleased $2\mu\text{m}$ -width resistor. However, for all three cases, at high frequency above 5 MHz, input power required to generate a bubble continuously increases with respect to frequency.

INTRODUCTION

Micro actuators using thermally generated bubbles have advantages over existing micro actuation mechanisms such as electrostatic, piezoelectric, and thermal bimetallic because thermal bubble generation requires a relatively low power input ($<100\text{mW}$) and generate large displacements and forces [1,2,3].

However, past works have been focused on thermal bubble generation using DC power input [2,3,4]. AC inductive telemetric powering is an alternative to traditional DC powering, which requires lead wires. It can potentially reduce the complexity of MEMS package and increase reliability. Since an oscillating electromagnetic field can penetrate media such as air and tissues, it is capable of providing

power to miniaturized MEMS units. In recent decades, telemetric signal transfer and powering of integrated circuits have been actively studied by biomedical researchers for embedded sensors [5,6]. Also, MEMS devices with the telemetry system are useful for harsh working environment such as high temperature in turbine engines and compressors, since it requires no physical contact with the sensor and no active elements such as power supplies, transistors and batteries [7].

In order to realize the telemetric powered micro bubbling, frequency response and heating behavior of the liquid need to be investigated first. Since significant power transfer is limited by the size of inductors, it must be found conditions for reducing power requirement.

DESIGN

Thermal bubble generation is demonstrated using the micro heater fabricated with polysilicon structure on phosphorous silicate glass (PSG) which serves as a sacrificial layer and dielectric layer. Fig. 1 shows the current design of the polysilicon heater. The micro heaters are $40\mu\text{m}$ -long, and $0.5\mu\text{m}$ -thick. One is $2\mu\text{m}$ width and the other $6\mu\text{m}$ width. They exhibit a sheet resistivity of $50 \Omega/\text{square}$. Nominal resistances are $1 \text{K}\Omega$ and $0.33 \text{K}\Omega$ for $2\mu\text{m}$ and $6\mu\text{m}$, respectively. By changing the width of the heater, we can have not only different values of the nominal resistance but also the surface area of the heater. In order to reduce the power requirement, we limit the width of the heater at $6\mu\text{m}$ since the wider the width of the resistor becomes the more power will be required to generate a bubble.

When the resistor is submerged in a liquid, power is applied. Heated liquid starts to form vapor as local heating occurs. Evaporation occurs when the surface temperature, T_s exceeds the saturation temperature, T_{sat} that corresponds to the liquid pressure [8]. Heat transfer from the solid surface to the liquid is a function of the surface area and excess temperature, and can be defined by the Newton's law of cooling as following.

$$q_s = hA(T_s - T_{\text{sat}}) = hA\Delta T_e \quad (1)$$

where, q_s = heat transfer from the heater to liquid
 h = convection coefficient

A = surface area of the heater
 ΔT_e = excess temperature

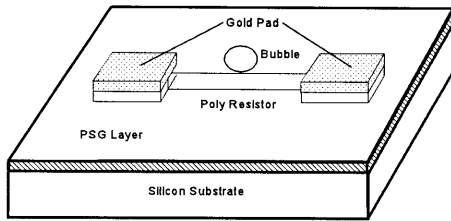


Figure 1. Diagram of the polysilicon heater design.

FABRICATION

The fabrication process (Fig. 3) starts with the deposition of $2\mu\text{m}$ of PSG and $0.5\mu\text{m}$ of polysilicon using LPCVD. Then, phosphorous ion implantation doping is done on the polysilicon layer. Doping concentration is $10^{16}/\text{cm}^2$. In order to activate and distribute the dopant, the sample is annealed at 1000°C for an hour. After that, 2000 \AA thick gold film is deposited (Fig. 3a). First this gold film is patterned for the electrical contact pad (Fig. 3b). Next, polysilicon is patterned using Freon 14 RIE etching (Fig. 3c). Polysilicon resistor can be released in 49% HF for 30 sec (Fig. 3d).

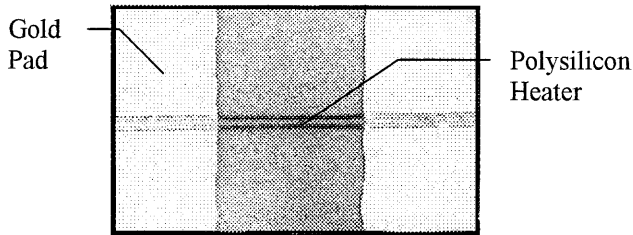


Figure 2. polysilicon heater.

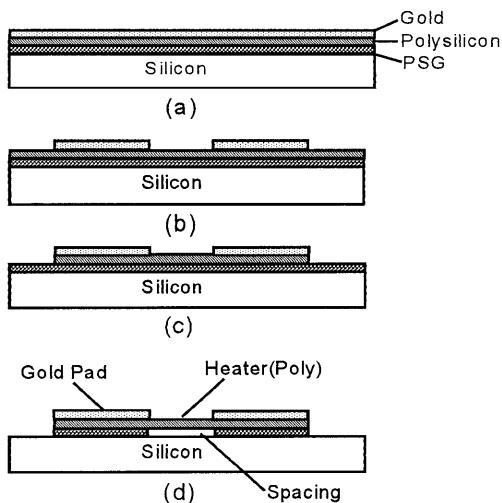


Figure 3. Process flow.

BUBBLE GENERATION MECHANISM

In order to generate a bubble, the resistor is completely immersed in initially stagnant liquid. This is the case of saturated pool boiling. In the pool boiling, when the temperature of the heater exceeds the saturation temperature of the liquid by a sufficient amount, vapor bubble nucleation occurs on the surface of the heater as the liquid is superheated.

There are two major types of nucleation [9]. First, nucleation can occur in a pure liquid. Second, nucleation happens on a foreign object, which can be a cavity on the heating wall or suspended foreign material with a nonwetted surface. The first nucleation mechanism can be categorized into homogeneous and heterogeneous nucleations. Homogeneous nucleation occurs within a superheated region of the liquid. On the contrary, heterogeneous nucleation occurs at the interface of a liquid and the heater surface. Since micromachining might produce a rough surface, it might generate a large enough cavity which can act as a nucleation site. In our study, we observed that nucleation always occurs at the same location of the resistor.

EXPERIMENTS

Tests were conducted at room temperature and atmospheric pressure under a probe station. For the resistor with the dimension of $40 \times 2 \times 0.5\mu\text{m}$, tests of bubble generation were conducted both before and after the removal of the PSG sacrificial layer, which also serves to conduct heat from the resistive heating element to the substrate (heat sink). We tested thermal bubble generation in isopropanol alcohol solution (IPA) which is a non-conductive liquid. Frequency used for testing ranges from 1 Hz to 15 MHz. Fig. 4 shows the circuit diagram for electric characterization test. We find out the relationship between the input power and the actual power applied to the resistor to find electrical characteristics of the system. This is shown in Fig. 5.

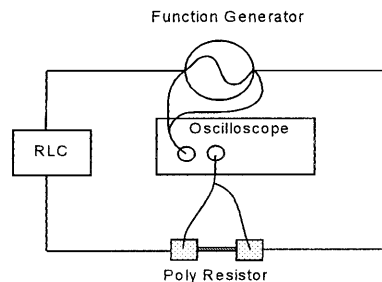


Figure 4. Circuit to measure input voltage and actual applied voltage to the resistor.

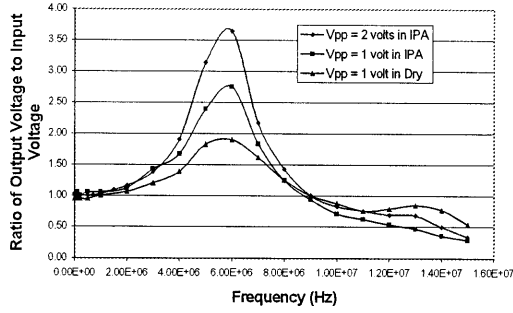


Figure 5. The ratio of the actual applied voltage to the input voltage. The RLC network behaves as a band pass filter

RESULTS and ANALYSIS

First, DC measurement of bubble generating power was conducted. Bubble generation can be easily detected under a microscope. As soon as we see the formation of a bubble, we record the input voltage of the power source. The measured threshold power to form a bubble was 67 mW for an unreleased resistor and 44 mW for the released for the case of 2 μm -width resistor. For the 6 μm , threshold power for DC input was 38 mW. This is expected based on the theory of the heat transfer and nucleation. The measured I-V curve of the resistor in air (Fig. 5) indicates the extent of heating on the resistor, which has temperature coefficient of resistance (TCR) on the order of 0.13%. This is more explicitly shown in Fig. 6. This curve follows the eq. (1), the greater heat transfer is, which is applied power, to the resistor, the larger the temperature of the resistor is.

AC signal varying from 1Hz up to 15MHz, is applied to the heater to characterize the frequency response of bubble generation in IPA. The result is shown in Fig. 7 to 9. On the basis of the DC input results and the theory, we expected relatively constant power input to generate a bubble over a range of frequency. As it can be seen from the Fig. 7, higher power is required to generate a bubble as the input frequency of AC signal increases. Minimum threshold power is observed at around 5.3 MHz. We define this frequency as f_{opt} and the threshold power as P_{min} at this frequency. It is measured that P_{min} is 36 mW for unreleased resistor and 20 mW for the released one (Fig. 8). The span of the valley is 1.2 MHz around the f_{opt} . Around the frequency of 4 MHz, threshold power becomes the highest value. However, this feature is not shown in the released resistor. These kinds of input power behavior is related to the dynamics of thermal transfer of the resistor tested, the super-heated liquid surrounding the resistor, the bulk of

subcooled IPA, and electrical characteristic. This suggests an optimal operating frequency band for the telemetry application. However, this kind of behavior is not expected based on the theory and past works using DC power input.

In addition to the frequency dependency, we also find the threshold power is subjected to the waveform of the AC signals. It is shown from Fig. 7. that the square wave is more efficient in terms of power consumption to generate bubble compared with the sine wave. At 5.3 MHz, the P_{min} is 36 mW for square wave and 57 mW for sine wave.

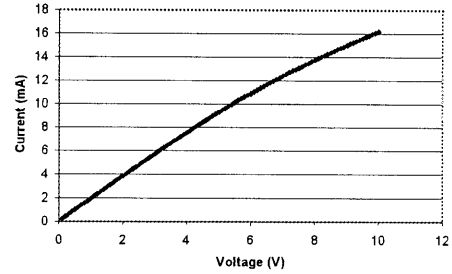


Figure 6. I-V curve of the heater measured in air, $TCR = 0.13\%$.

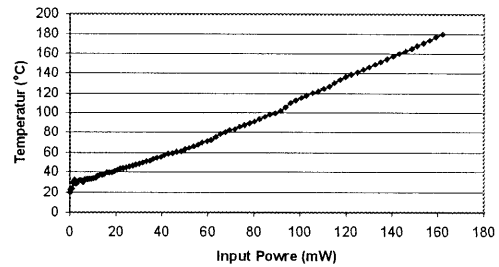


Figure 7. Temperature of the resistor increases as the input power increases.

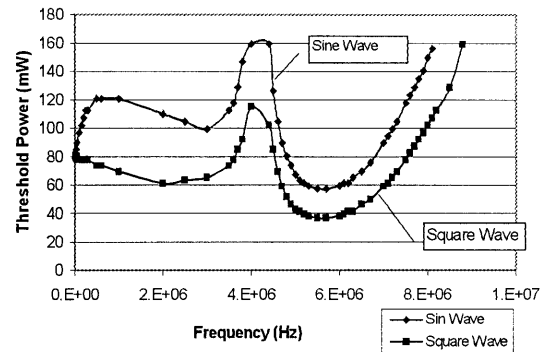


Figure 8. Frequency response shows the power valley at 5.3 MHz. A square wave requires lower power input.

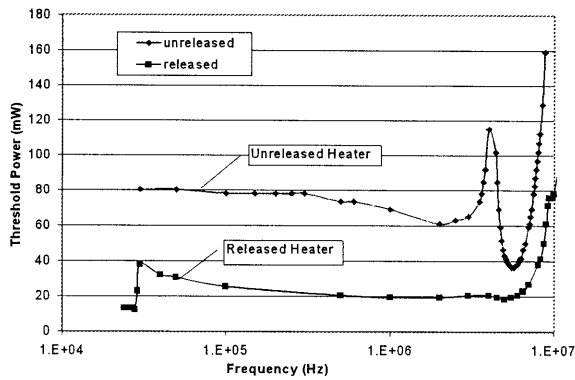


Figure 9. Power reduction by releasing the resistor from the substrate. P_{min} is reduced from 36 to 20 mW.

In order to find the relationship between the input power and dimension (width of the resistor), we fabricated another resistor with the same length and thickness, but with a different width. It has the dimension of $40 \times 6 \times 0.5 \mu\text{m}$. Fig. 9. shows the input power behavior with respect to frequency. Test was done by using sine wave under the same condition as the previous test. The resistor is not released from its substrate. When we compare Fig. 7 and 9, $6 \mu\text{m}$ -width resistor does not have a high peak around 4 MHz. However, both cases have the same trend at high frequency, 6 MHz for the $2 \mu\text{m}$ and 8 MHz for the $6 \mu\text{m}$. When we compare released case in Fig. 8 with Fig. 9, we can find very similar behavior. In both cases, input power remains constant frequency below 8 MHz, and starts to increase above that frequency with respect to frequency.

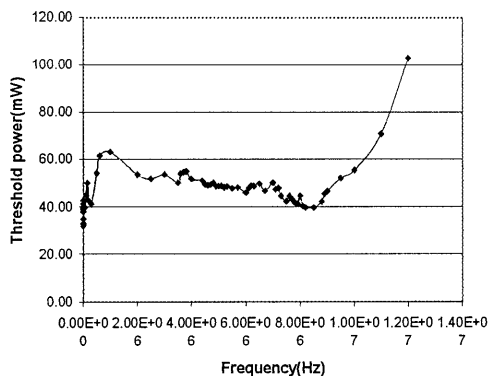


Figure 10. Threshold power of the resistor with $6 \mu\text{m}$ width. It does not have a peak at $f = 4 \text{ MHz}$.

CONCLUSIONS

Characterizations of bubble generation using AC bias have been demonstrated. Unlike the case of DC power input, AC power input shows very unique

features such as dependency of input wave form, dimension, and the structure of the resistor. These features might be due to the effect of the electrical characteristics of the device. Yet, more research has to be done to understand the physics behind of the bubble generation using AC power input, and to verify the results presented in this paper. This research is the starting point of the more rigorous investigation of the bubble generation under AC bias. Since the bubble generation under AC bias has a great potential, and remains relatively unexplored, this gives us the optimism for further research on the subject.

ACKNOWLEDGEMENT

This project is funded by DARPA under Composite Cad. Contract number is F30602-98-20178.

REFERENCES

- [1] X. Yang, C. Grosjean, Y. C. Tai, and C.M. Ho, "A MEMS Thermo-neumatic Silicone Membrane Valve," *MEMS '97*, p.114, 1997.
- [2] L. Lin, A.P. Pisano, and A.P. Lee, "Micro-bubble Powered Actuator," *Transducer '91*, p. 1041.
- [3] L. Lin, A.P. Pisano, V.P. Carey, "Thermal Bubble Formation on Polysilicon Micro resistors," *Journal of Heat Transfer-Transactions of the ASME*, vol.120, no.3, Aug. 1998, pp.735-42.
- [4] T. Jun, C.J. Kim, "Microscale Pumping with Traversing Bubbles in Microchannels," *Solid-State Sensors and Actuators Workshop (Hilton Head Workshop)*, Hilton Head, 1996.
- [5] M. Shah, R. Phillips, and R. Norman, "A Study of Printed Spiral Coils for Neuroprosthetic Transcranial Telemetry Application," *IEEE Transactions on Biomedical Engineering*, Vol 45, No. 7, July 1998, pp. 867-875.
- [6] T. Akin, B. Ziaie, K. Najafi, "RF Telemetry Powering and Control of Hermetically Sealed Integrated Sensors and Actuators," *IEEE Solid-State Sensor and Actuator Workshop*, IEEE 1990, pp145-8.
- [7] J.M. English and M.G. Allen, "Wireless Micromachined Ceramic Pressure Sensors," *MEMS '99*, Orlando, Florida, USA, Jan 17-21,1999, pp. 511-516.
- [8] F.P. Incropera and D.P. DeWitt, *Introduction to Heat Transfer*, New York, 1996 John Wiley & Sons.
- [9] L.S. Tong and Y.S. Tang, *Boiling Heat Transfer and Two-Phase Flow*, Washington, 1997 Taylor & Francis.